中国光学（中英文） Chinese Optics 核心期刊

Influencing factor of the characterization and restoration of phase aberrations resulting from atmospheric turbulence based on Principal Component Analysis

WANG Jiang-pu-zhen, WANG Zhi-qiang, ZHANG Jing-hui, QIAO Chun-hong, FAN Cheng-yu

Citation:
WANG Jiang-pu-zhen, WANG Zhi-qiang, ZHANG Jing-hui, QIAO Chun-hong, FAN Cheng-yu. Influencing factor of the characterization and restoration of phase aberrations resulting from atmospheric turbulence based on Principal Component Analysis[J]. *Chinese Optics*, 2025, 18(4): 899-907. doi: 10.37188/CO.EN-2024-0035
王姜菩真, 王志强, 张京会, 乔春红, 范承玉. 基于主成分分析法的大气湍流相位畸变表征和还原影响因素分析[J]. 中国光学, 2025, 18(4): 899-907. doi: 10.37188/CO.EN-2024-0035

View online: https://doi.org/10.37188/CO.EN-2024-0035

Articles you may be interested in

White light interferometry micro measurement algorithm based on principal component analysis
基于主成分分析的白光干涉微观形貌测量算法
Chinese Optics. 2023, 16(3): 637 https://doi.org/10.37188/CO.2022-0172

Effect of atmospheric turbulence on the tracking accuracy of high-resolution remote sensing satellites
大气湍流对高分辨率遥感卫星定位精度的影响分析
Chinese Optics. 2023, 16(3): 550 https://doi.org/10.37188/CO.2022-0196

Suppression of the influence of atmospheric turbulence during the propagation of a twisted Laguerre-Gaussian correlated beam
扭曲拉盖尔—高斯关联光束对大气湍流传输影响的抑制
Chinese Optics. 2021, 14(3): 704 https://doi.org/10.37188/CO.2020-0138

Analysis of effects on the beam quality β factor of high power laser
高能激光光束质量β因子的影响因素分析
Chinese Optics. 2021, 14(2): 353 https://doi.org/10.37188/CO.2020-0137

Applications of GFC-IFC in trace multi-component gas analysis
GFC-IFC技术在多组分微量气体分析中的应用
Chinese Optics. 2021, 14(6): 1378 https://doi.org/10.37188/CO.2021-0064

Research progress of aberration analysis and imaging technology based on metalens
超表面透镜的像差分析和成像技术研究
Chinese Optics. 2021, 14(4): 831 https://doi.org/10.37188/CO.2021-0014

文章编号 2097-1842(2025)04-0899-09

Influencing factor of the characterization and restoration of phase aberrations resulting from atmospheric turbulence based on Principal Component Analysis

WANG Jiang-pu-zhen[1,2,3], WANG Zhi-qiang[1,3 *], ZHANG Jing-hui[1,4], QIAO Chun-hong[1,4], FAN Cheng-yu[1,3 *]

（1. *Key Laboratory of Atmospheric Optics*, *Anhui Institute of Optics and Fine Mechanics*, *HFIPS*, *Chinese Academy of Sciences*, *Hefei* 230031, *China*;

2. *Science Island Branch of Graduate School*, *University of Science and Technology of China*, *Hefei* 230026, *China*;

3. *Nanhu Laser Laboratory*, *National University of Defense Technology*, *Changsha* 410073, *China*;

4. *State Key Laboratory of Laser Interaction with Matter*, *Anhui Institute of Optics and Fine Mechanics*, *HFIPS*, *Chinese Academy of Sciences*, *Hefei* 230031, *China*）

* *Corresponding author*, *E-mail*: *zqwang@aiofm.ac.cn*; *cyfan@aiofm.ac.cn*

Abstract: Restoration of phase aberrations is crucial for addressing atmospheric turbulence in light propagation. Traditional restoration algorithms based on Zernike polynomials (ZPs) often encounter challenges related to high computational complexity and insufficient capture of high-frequency phase aberration components, so we proposed a Principal-Component-Analysis-based method for representing phase aberrations. This paper discusses the factors influencing the accuracy of restoration, mainly including the sample space size and the sampling interval of D/r_0, on the basis of characterizing phase aberrations by Principal Components (PCs). The experimental results show that a larger D/r_0 sampling interval can ensure the generalization ability and robustness of the principal components in the case of a limited amount of original data, which can help to achieve high-precision deployment of the model in practical applications quickly. In the environment with relatively strong turbulence in the test set of $D/r_0 = 24$, the use of 34 terms of PCs can improve the corrected Strehl ratio (SR) from 0.007 to 0.158 5, while the Strehl ratio of the light spot after restoration using 34 terms of ZPs is only 0.021 5, demonstrating almost no correction effect. The results indicate that PCs can serve as a better alternative in representing and restoring the characteristics of atmospheric turbulence induced phase aberrations. These findings pave the way to use PCs of phase aberrations with fewer terms than traditional ZPs to achieve data dimensionality reduction, and offer a reference to accelerate and stabilize the model and deep learning based adaptive optics correction.

Key words: phase aberration; atmospheric turbulence; principal component analysis; Zernike polynomials

收稿日期:2024-11-14; **修订日期**:2024-12-11

基金项目:国家自然科学基金资助项目（No. 12273084）; 中国科学院重点实验室科技创新项目（No. CXJJ-225028）

Supported by the National Natural Science Foundation of China (No. 12273084); Science and Technology Innovation Fund for Key Laboratories of the Chinese Academy of Sciences (No. CXJJ-225028)

基于主成分分析法的大气湍流相位畸变表征和还原影响因素分析

王姜菩真[1,2,3], 王志强[1,3*], 张京会[1,4], 乔春红[1,4], 范承玉[1,3*]

（1. 中国科学院合肥物质科学研究院安徽光学精密机械研究所 中国科学院大气光学重点实验室, 安徽 合肥 230031；
2. 中国科学技术大学研究生院科学岛分院, 安徽 合肥 230026；
3. 南湖之光实验室, 中国人民解放军国防科技大学, 湖南 长沙 410073；
4. 激光与物质相互作用全国重点实验室, 中国科学院合肥物质科学研究院安徽光学精密机械研究所, 安徽 合肥 230031）

摘要: 为了有效表征、还原大气湍流造成的相位畸变, 解决传统 Zernike 多项式方法引起的相位还原高频信息不足问题, 提出了基于主成分分析法的畸变相位特征表征、还原方法, 对可能影响主成分精度从而影响还原效果的因素进行研究。首先建立了几组包含满足 Von-Karman 功率谱畸变相位的原始数据集, 并生成了 D/r_0 采样间隔分别为 1 和 10 的样本空间。接着, 建立了不同湍流强度下畸变相位的测试集数据。之后从不同原始数据集中提取对应的主成分, 并分别使用相同项数的主成分与 Zernike 多项式对同一组测试集畸变相位进行还原。最终对比还原结果, 分析原始数据样本量和 D/r_0 采样间隔对主成分精度的影响。实验结果表明: 更大的 D/r_0 采样间隔可以在原始数据量有限的情况下保证主成分的泛化能力和鲁棒性, 从而在实际应用中快速实现模型的高精度部署; 在测试集 D/r_0=24 的相对湍流较强的环境下, 使用 34 阶主成分可以将校正后光斑 Strehl 比从原始的 0.007 提升至 0.1585, 而同样使用 34 阶 Zernike 还原后的光斑 Strehl 比仅为 0.0215, 几乎没有校正效果。可以看出基于主成分分析法的大气湍流相位畸变表征和还原方法优于 Zernike 多项式法, 可以为基于模型和深度学习的自适应光学校正提供参考。

关　键　词: 相位畸变; 大气湍流; 主成分分析法; Zernike 多项式

中图分类号: TP394.1;TH691.9　**文献标志码:** A　**doi:** 10.37188/CO.EN-2024-0035　**CSTR:** 32171.14.CO.EN-2024-0035

1 Introduction

Atmospheric turbulence can affect the quality of light waves, thereby impacting the clarity and resolution of astronomical observations and the transmission of free-space optical communications[1-2]. Adaptive optics technology was therefore proposed to correct phase aberrations caused by atmospheric turbulence using efficient wavefront sensing[3-4].

The traditional Shack–Hartmann wavefront sensor and the shearing interferometer have problems that prevent them from restoring phase distortion very well. The Shack–Hartmann wavefront sensor can only measure the phase aberration with limited spatial resolution because of the sub-aperture constriction[5-6]. The shearing interferometer splits the beam into two wavefronts, lowering the light energy utilization efficiency and subsequently reducing the accuracy of wavefront sensing[7-8]. In recent years, image-based wavefront sensing has gained attention. With the help of deep learning (DL), wavefront reconstruction is now much more efficient and accurate[9-12]. Paine *et al*[13] predicted Zernike polynomials (ZPs) coefficients from a computational simulated point spread function (PSF) using a convolutional neural network (CNN) for wavefront reconstruction in 2018. Nishikazi *et al*[14] experimentally verified the effectiveness of CNN in predicting coefficients of ZPs and estimating wavefront aberrations in 2019. Ge *et al*[15] further used a DL network to achieve high-precision mapping of phase features to wavefront aberrations in phase re-

construction in 2024.

Most image-based wavefront sensing methods use ZPs, a classic way to represent phase aberrations, as mentioned above. The higher the term of ZPs used, the more high-frequency components captured, and the more accurate the restoration of phase aberrations[16]. However, using more ZPs makes the computer work harder, making predictions by the CNN model less accurate[17], while using fewer ZPs reduces the model's generalization ability to deal with complex environments such as strong turbulence.

The statistical Principal Component Analysis (PCA) method is becoming popular. PCA can identify the most dominant features from a large dataset. Over the past few years, researchers have successfully applied PCA to reduce speckle noise[18], denoise meteorological echoes[19], and combine with neural networks to correct non-common path aberrations[20].

Inspired by the successful implementation of PCA, we performed PCA in the representation of phase aberrations caused by atmospheric turbulence and proved its validity. This paper discusses the factors affecting the restoration accuracy by principal components (PCs), mainly including the size of sample space and sampling interval of D/r_0 on the basis of characterizing phase aberrations by PCs. Section 2 provides a basic overview of the method used in the paper, and Section 3 introduces the simulation process. Section 4 verifies the representation and restoration performance of the PCA method and compares with the traditional ZPs method. Our analysis demonstrates that the PCA method outperforms traditional ZPs across varying atmospheric turbulence strengths, especially in challenging situations such as strong turbulence, providing a statistical reference for data acquisition for PCs model deployment in real applications.

2 Methods

To simulate atmospheric turbulence accurately, we created a phase screen data set that satisfies the modified Von Karman power spectrum using the Fast Fourier Transform[21], and the inner and outer scales of atmospheric turbulence were set as 0.005 m and 10 m. According to Noll[22], the phase aberration $W(\rho,\theta)$ can be represented as a combination of ZP $Z_j(\rho,\theta)$ with coefficients a_j. This paper ignores the first three terms of ZPs, which do not change the morphology of the aberration, and focuses on the aberration above the 4th term: defocus. As ZP patterns are generally grouped in terms of spherical aberration, it is generally accepted that aberration patterns before the tertiary spherical aberration carry more weight and that using more terms increases the computational burden. Still, the improvement in aberration restoration is not significant. So, the 4th to 37th ZPs (tertiary spherical aberrations) were used to fit the original phase aberration and set the piston, x tilt, and y tilt terms to 0 to generate a new phase aberration dataset, as shown in the following expression:

$$W_1(\rho,\theta)=\sum_{j=4}^{37}a_jZ_j(\rho,\theta) \quad , \qquad (1)$$

where ρ and θ are the radial and azimuthal variables in a polar coordinate. ZPs have a specific pattern for each term, with more information in higher terms. More terms allow the phase aberration to be restored more finely, but it is slower and less efficient. A few terms are therefore often used, but higher frequencies are often missed. We propose the PCA method, a useful statistical tool for reducing multiple complex variables, to represent and restore the phase aberrations. The old variables are combined to form new variables as:

$$\boldsymbol{y}_i=\boldsymbol{V}'\boldsymbol{x}_i \quad , \qquad (2)$$

where $\boldsymbol{V}$ is the transformation matrix and the symbol $'$ means transpose of the vector or the matrix. where $\boldsymbol{y}_i=(y_{1i},y_{2i},\cdots,y_{ni})'$ is the new variable, and $\boldsymbol{x}_i=(x_{1i},x_{2i},\cdots,x_{ni})'$ is the original variable. This approach keeps the information in lower- and higher-term components in each new single mode. The

first m new variables with the highest variance, i.e., the PCs, are selected to distill the essence of the original dataset. This summary shows the main features of the original data and reduces the number of dimensions. To be consistent with Eq.(1) above, the representation of the phase aberration fitted using the first 34 terms of PCs is shown below:

$$W_2(r,q)=\sum_{j=1}^{34}(b_j PC_j) \quad , \qquad (3)$$

where PC_j is the j^{th} PC term with coefficient b_j. To analyze the validity of PCA in different conditions, we need to create datasets that show different turbulence levels. Based on Lane's derivation[23], D/r_0 is used to characterize the strength with r_0 being the atmospheric coherence length and D being the pupil diameter. The numerical interval is D/r_0 from 1 to 30. 1−10 is relatively weak turbulence, 10−20 is medium, and 20−30 is relatively strong. Further, the PSF's Strehl ratio (SR) is used to evaluate the effectiveness of phase restoration by performing a fast Fourier transform on the residual phase aberration.

3 Simulation

This paper focuses on analyzing factors influencing the accuracy of PCs restoration of phase aberration: the original phase data's sample space size and the sampling interval of D/r_0. In order to conduct a more comprehensive analysis of PCs' restoration effectiveness in different propagation conditions, generating phase datasets that can encompass different turbulence strengths is necessary.

The simulation was performed according to the following steps:

(1) The original sample space was randomly generated containing N distorted phases, then a PCA was performed on the base data to generate the PCs. N = 5 000, 10 000, and 30 000 were chosen.

(2) For the equivalent sample space size, two sample spaces were generated with different D/r_0 sampling intervals. Space A had an average distribution between 1−30, while space B had D/r_0=5, 15, and 25 as representative values of weak, medium and strong turbulence, respectively. A PCA was performed on both datasets A and B to extract corresponding PCs.

(3) The phase aberrations of the test set were restored under different turbulence strengths using 8, 19, 34 terms of ZPs and PCs obtained from different sample spaces. The terms employed were based on the Zernike primary, secondary, and tertiary spherical aberrations (11th, 22nd, and 37th). That is, using the ZPs starting from the 4th term of defocus and ending with the spherical aberration term, a total of 8, 19, and 34 terms of modes were included. The restoration effects of the two methods were compared.

4 Results

Fig. 1 (color online) shows the restoration effects of equivalent terms of ZPs and PCs obtained from A-5000, A-10000, and A-30000 datasets. In order to provide a comprehensive demonstration of the restoration effects, we took test sets of D/r_0= 8, 16, and 24, and restoration was performed using the first 8, 19, and 34 terms PCs and ZPs, respectively. The terms employed start with 4th ZP: defocus, and end with the Zernike primary, secondary, and tertiary spherical aberrations (11th, 22^{nd,} and 37th). Fig. 1 shows the positive correlation between the original data amount and the PCs' restoration effect. When 5 000 sets of original phase data are used, the advantage of PCs may not be immediately apparent. The corrected SR obtained using 8 terms of PCs obtained from 5 000 sets of original data in Fig. 1(a) is only slightly higher than SR obtained by ZPs; as the amount of original data increases, the accuracy of PCs improves, and the gap with ZPs gradually widens. When using the PCs generated from 30 000 sets of original data, the corrected spot is clear and bright as shown in Fig. 1(c), where the turbulence is stronger and the SR can reach 0.218 3. At this point, the SR after restoration using PCs obtained from

5 000 sets is 0.156 1, while the SR after restoration using equivalent terms of ZPs is only 0.117 1. It can be seen that the advantage of PCs is more significant under strong turbulence, showing that PCs are stable and consistent and can adapt to different environments.

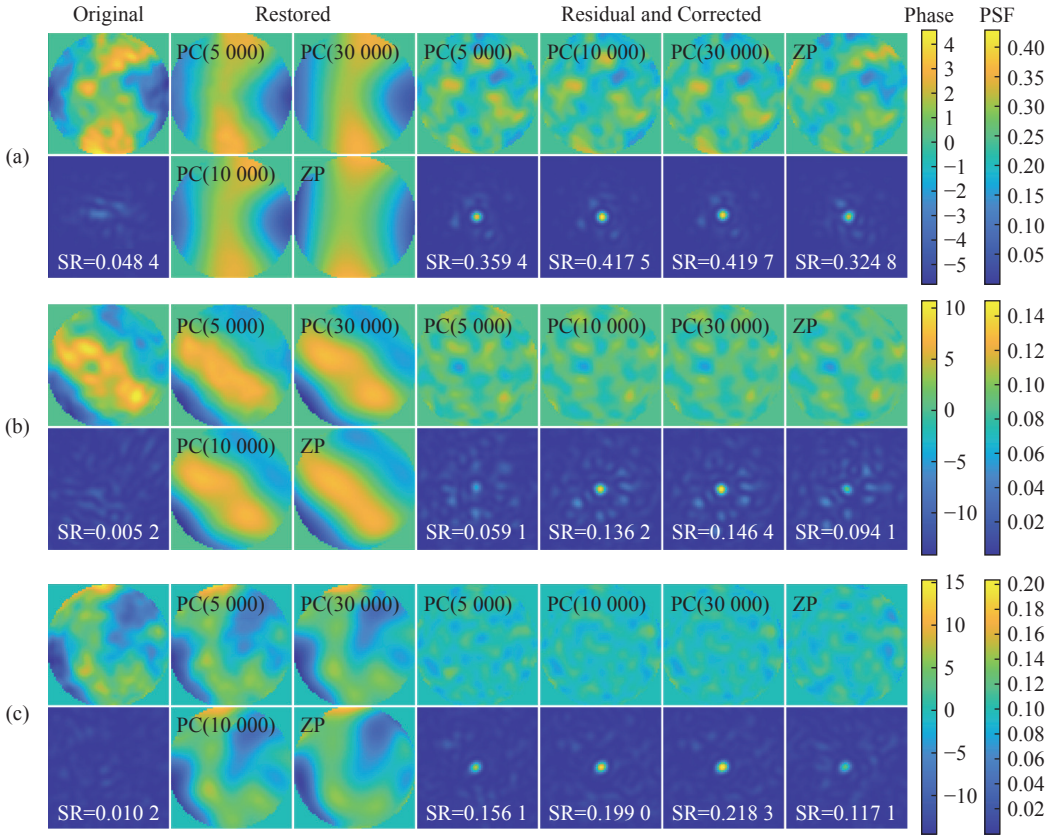

Fig. 1 Examples of restoration of phase aberration by ZPs vs PCs obtained from different sample space sizes under the same turbulence strength. (a) $D/r_0 = 8$,using the first 8 terms; (b) $D/r_0 = 16$, using the first 19 terms; (c) $D/r_0 = 24$,using the first 34 terms

Furthermore, Fig. 2 (color online) shows the effect of using different amounts of terms of PCs to restore the same phase aberration under the same turbulence strength. The PCs used were extracted from 30 000 sets of original data. Combined with Fig. 1, it shows that under weak turbulence, the phase aberration can be effectively restored using only 8 terms of PCs, and the corrected SR reaches 0.413 1, further indicating that the PCs can effectively extract the main features of the phase aberrations; under medium turbulence, the aberration can be effectively restored using 19 terms of PCs, and under strong turbulence, the phase aberration can still be stably restored using 34 terms of PCs, and the corrected SR is about 0.2. This result again shows that PCs have the robustness to manage different levels of environmental turbulence and may be more suitable than ZPs for working under challenging conditions.

Fig. 3 (color online) further explores the mean SR after restoring phase aberrations at different turbulence strengths using equivalent terms of ZPs and PCs that were extracted from different sample spaces. It shows that the PCs obtained from the 30 000 sets of original phase data are the most effective in restoring the phase aberrations. This is because the larger the data volume, the broader the model. Notably, PCs from 10 000 sets (blue triangular scatter lines) and 30 000 sets (orange circular scatter lines) almost overlap in Fig. 3, suggesting sample space size has limited impact. If the original data already covers enough phase information, adding more

sample data won't significantly improve the accuracy of PCs, but will just add redundant data, which will hinder the rapid deployment of models in real-world applications. This provides an important basis for model optimization of PCs in practical applications.

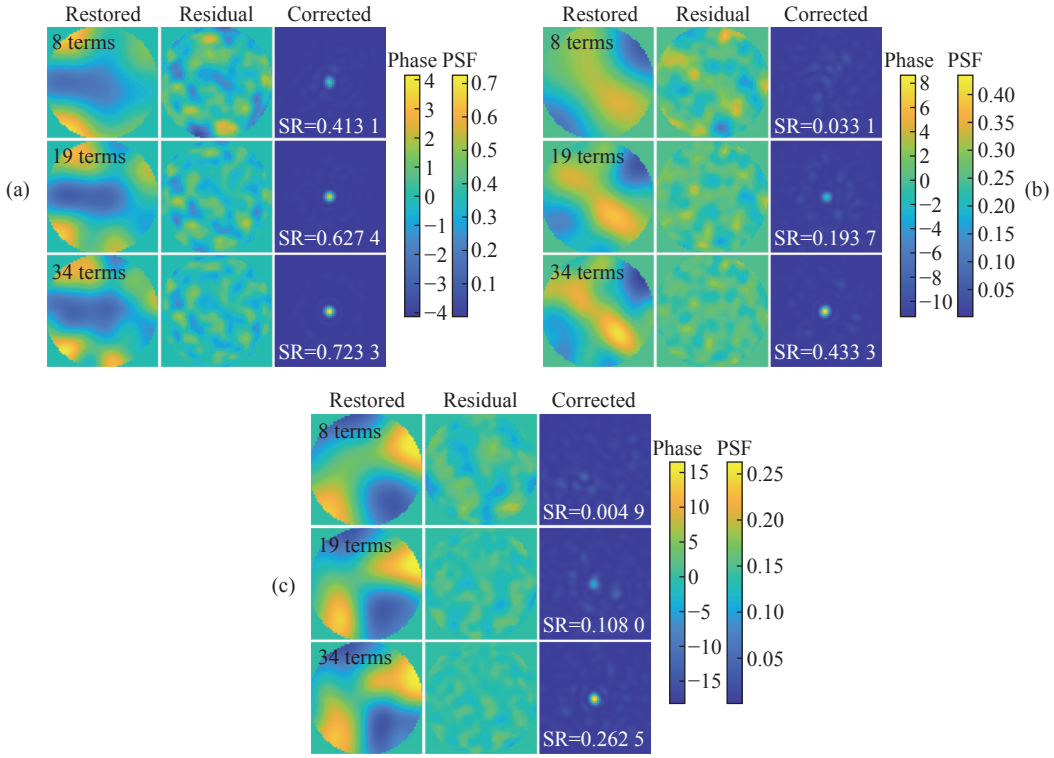

Fig. 2 Examples of restoration by 8, 19, and 34 PCs. (a) $D/r_0 = 8$; (b) $D/r_0 = 16$; (c) $D/r_0 = 24$

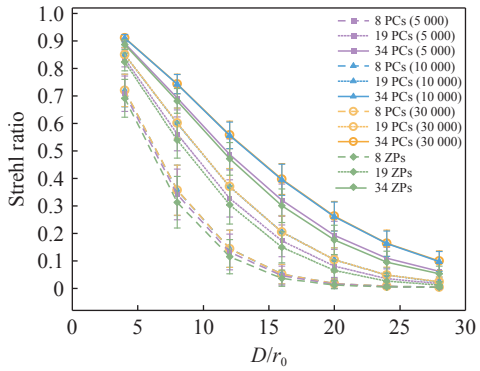

Fig. 3 Mean SR after phase aberration restoration by ZPs vs PCs obtained from different sizes of sample spaces under different turbulence scenarios

Although increasing the size of the sample space can improve the accuracy of PCs, it can also increase the computational and time costs. In the actual model deployment, it's desirable to obtain the most accurate PCs of the phase aberrations caused by the local atmospheric turbulence with the shortest possible sampling time. The D/r_0 sampling interval was increased from 1 in *A*-space to 10 in *B*-space to analyze the impact of the sampling interval on the accuracy of the PCs. Fig. 4 compares the restoration for the same phase aberrations by PCs obtained from *A*-5000 and *B*-5000. It demonstrates that PCs obtained from the *B*-5000 with larger sampling intervals are significantly better for restoration than those from the *A*-5000.

Tab. 1 compares the restoration by PCs from *B*-5000 and *A*-30000, demonstrating that when the sampling interval is increased, the accuracy of the PCs obtained from only 5 000 sets of sampled data can be comparable to that obtained from 30 000 sets of sampled data.

This is because when the sampling interval is increased, the number of sampling points is reduced, and the size of the sample space corresponding to a single sampling point is increased, enabling the dataset to contain more varied information in a wider range. Therefore, when it is necessary to deploy the PCs model quickly for restoration, the

sample space size can be reduced and the sampling interval can be increased to ensure the model's generalization ability and robustness while minimizing the data's redundancy.

Fig. 5 (color online) shows some examples of restoration by PCs generated from the *B*-5000 and ZPs of equivalent terms. Fig. 5(c) indicates that PCs are more effective than ZPs for restoring phase aberration in challenging environments, such as strong turbulence. Using the first 34 terms, the SR of the PSF after restoration by PCs reached 0.158 5, which meets the requirements of engineering applications. At this time, the SR of the PSF after restoration by ZPs is only 0.02, and compared with the SR of the original spot PSF, which is 0.007, the effect of the ZP for restoration is almost negligible. This shows that PCs perform better, further supporting the stability of PCs demonstrated in Fig. 1 and 3.

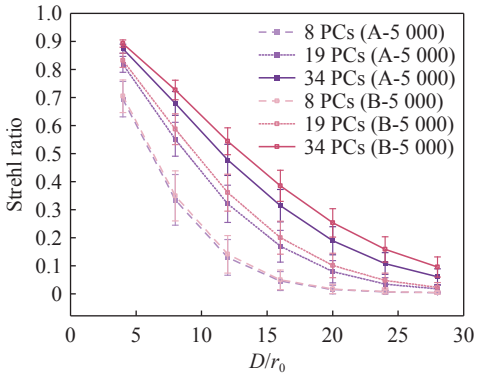

Fig. 4　Comparison of the mean Strehl ratio after phase aberration restoration by PCs obtained from *A*-5000 and *B*-5000

Tab. 1　Comparison of the mean Strehl ratio after phase restoration by PCs obtained from *B*-5000 and *A*-30000 (The first row 4-28 indicates the D/r_0 of test sets)

Terms		D/r_0						
	N	4	8	12	16	20	24	28
8	5 000	0.719	0.356 3	0.143 7	0.051 5	0.017 7	0.007 2	0.004 6
	30 000	0.720 4	0.357 7	0.143 9	0.052 1	0.017 6	0.007 3	0.004 7
19	5 000	0.849 6	0.598 9	0.368	0.204	0.103	0.048 2	0.023 5
	30 000	0.850 5	0.601 1	0.370 2	0.204 9	0.104 1	0.048 8	0.024
34	5 000	0.910 1	0.741 2	0.554 7	0.392 5	0.258 2	0.161 6	0.097 8
	30 000	0.910 8	0.743 6	0.558 2	0.397 8	0.263 6	0.164 4	0.100 2

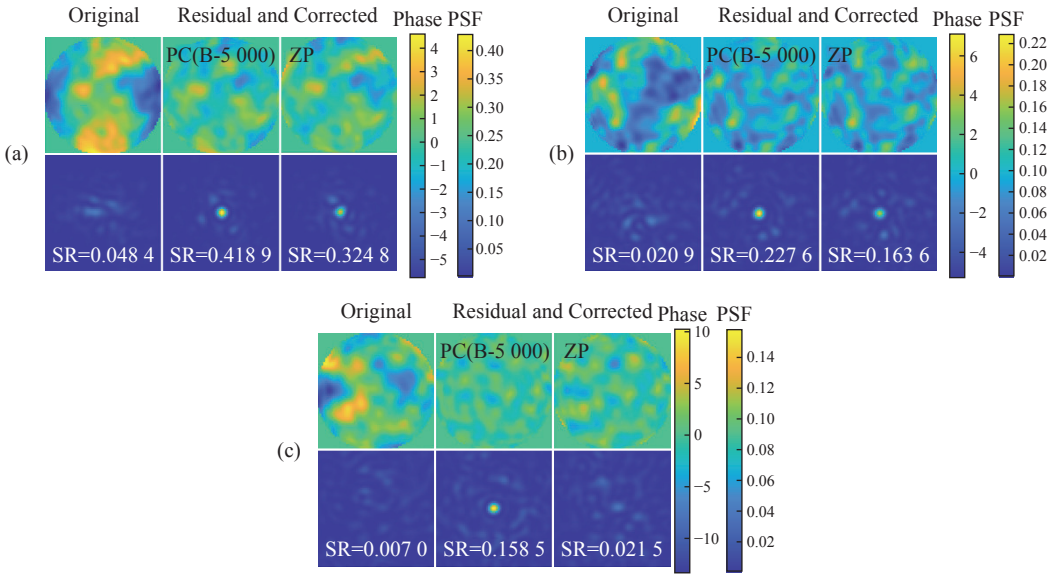

Fig. 5　Examples of restoration of phase aberrations by the equivalent terms of ZPs vs PCs obtained from *B*-5000. (a) $D/r_0 = 8$, using the first 8 terms; (b) $D/r_0 = 16$, using the first 19 terms; (c) $D/r_0 = 24$, using the first 34 terms

5 Conclusion

In this paper, the factors affecting the restoration accuracy of PCs, mainly sample space size and the D/r_0 sampling interval, are discussed in depth on the basis of characterizing phase aberrations by PCs. The results show that the more sample data, the higher the accuracy of the PCs and the better the adaptability in restoring phase aberrations in different environments. However, when the sample space contains enough phase information, a further increase in sample data no longer improves the accuracy of the PCs but results in data redundancy. When the model needs to be deployed quickly, the generalizability and robustness of PCs can be ensured by appropriately reducing the sample space size and increasing the sampling interval.

In general, our work demonstrates that the PCA method outperforms traditional ZPs across varying atmospheric turbulence strengths, especially in challenging situations such as strong turbulence, indicating that the PCA method can serve as a better alternative in restoring the phase aberrations induced by atmospheric turbulence. These findings may help to reduce data dimensionality, i.e., using PCs of phase aberrations with fewer terms than traditional ZPs, which can help improve model and deep learning based adaptive optics correction.

References:

[1] MAHAJAN V N. Aberrations of diffracted wave fields. I. Optical imaging[J]. *Journal of the Optical Society of America A*, 2000, 17(12): 2216-2222.

[2] ANGEL J R P, WIZINOWICH P, LLOYD-HART M, *et al*.. Adaptive optics for array telescopes using neural-network techniques[J]. *Nature*, 1990, 348(6298): 221-224.

[3] SANDLER D G, BARRETT T K, PALMER D A, *et al*.. Use of a neural network to control an adaptive optics system for an astronomical telescope[J]. *Nature*, 1991, 351(6324): 300-302.

[4] JIA P, MA M Y, CAI D M, *et al*.. Compressive Shack–Hartmann wavefront sensor based on deep neural networks[J]. *Monthly Notices of the Royal Astronomical Society*, 2021, 503(3): 3194-3203.

[5] HARTLIEB S, WANG ZH, RÜDINGER A, *et al*.. Large dynamic range Shack–Hartmann wavefront sensor based on holographic multipoint generation and pattern correlation[J]. *Optical Engineering*, 2024, 63(2): 024107.

[6] VOLKOV M V, BOGACHEV V A, STARIKOV F A, *et al*.. Numerical study of dynamic adaptive phase correction of radiation turbulent distortions and estimation of their frequency bandwidth with a Shack–Hartmann wavefront sensor[J]. *Atmospheric and Oceanic Optics*, 2022, 35(3): 250-257.

[7] LI P, TANG F, WANG X ZH. Relationship between shear ratio and reconstruction accuracy in lateral shearing interferometry[J]. *Optical Engineering*, 2020, 59(3): 034113.

[8] 宋金伟, 闵俊伟, 袁勋, 等. 基于二维朗奇相位光栅的四波横向剪切干涉定量相位成像[J]. 光子学报, 2022, 51(11): 1118001.
SONG J W, MIN J W, YUAN X, *et al*.. Quadriwave lateral shearing interferometry quantitative phase imaging based on 2D Ronchi phase grating[J]. *Acta Photonica Sinica*, 2022, 51(11): 1118001. (in Chinese).

[9] SINHA A, LEE J, LI SH, *et al*.. Lensless computational imaging through deep learning[J]. *Optica*, 2017, 4(9): 1117-1125.

[10] CHEN M A, JIN X Q, LI SH B, *et al*.. Compensation of turbulence-induced wavefront aberration with convolutional neural networks for FSO systems[J]. *Chinese Optics Letters*, 2021, 19(11): 110601.

[11] LOHANI S, GLASSER R T. Turbulence correction with artificial neural networks[J]. *Optics Letters*, 2018, 43(11): 2611-2614.

[12] GUO Y M, ZHONG L B, MIN L, *et al*.. Adaptive optics based on machine learning: a review[J]. *Opto-Electronic Advances*, 2022, 5(7): 200082.

[13] PAINE S W, FIENUP J R. Machine learning for improved image-based wavefront sensing[J]. *Optics Letters*, 2018, 43(6): 1235-1238.

[14] NISHIZAKI Y, VALDIVIA M, HORISAKI R, *et al*.. Deep learning wavefront sensing[J]. *Optics Express*, 2019, 27(1): 240-251.

[15] GE X L, ZHU L CH, GAO Z Y, *et al*.. Experimental demonstration of wavefront reconstruction and correction techniques for variable targets based on distorted grating and deep learning[J]. *Optics Express*, 2024, 32(10): 17775-17792.

[16] 王奇涛, 佟首峰, 徐友会. 采用 Zernike 多项式对大气湍流相位屏的仿真和验证[J]. 红外与激光工程, 2013, 42(7): 1907-1911.
WANG Q T, TONG SH F, XU Y H. On simulation and verification of the atmospheric turbulent phase screen with Zernike polynomials[J]. *Infrared and Laser Engineering*, 2013, 42(7): 1907-1911. (in Chinese).

[17] SIDDIK A B, SANDOVAL S, VOELZ D, *et al*.. Deep learning estimation of modified Zernike coefficients and recovery of point spread functions in turbulence[J]. *Optics Express*, 2023, 31(14): 22903-22913.

[18] LV H L, FU SH J, ZHANG C M, *et al*.. Speckle noise reduction of multi-frame optical coherence tomography data using multi-linear principal component analysis[J]. *Optics Express*, 2018, 26(9): 11804-11818.

[19] ZHANG Q, XIAO G, LAN Y Q, *et al*.. Atmospheric turbulence detection by PCA approach[J]. *Aerospace Systems*, 2019, 2(1): 15-20.

[20] TERRERI A, PEDICHINI F, DEL MORO D, *et al*.. Neural networks and PCA coefficients to identify and correct aberrations in adaptive optics[J]. *Astronomy & Astrophysics*, 2022, 666: A70.

[21] SCHMIDT J D. *Numerical Simulation of Optical Wave Propagation with Examples in MATLAB*[M]. Bellingham: SPIE, 2010.

[22] NOLL R J. Zernike polynomials and atmospheric turbulence[J]. *Journal of the Optical Society of America*, 1976, 66(3): 207-211.

[23] LANE R G, GLINDEMANN A, DAINTY J C. Simulation of a Kolmogorov phase screen[J]. *Waves in Random Media*, 1992, 2(3): 209-224.

Author Biographics:

WANG Jiang-pu-zhen (1998—), female, born in Jinan, Shandong Province, currently, as a doctoral candidate at University of Science and Technology of China (USTC). Her research interests are on the correction of phase aberrations resulting from atmospheric turbulence. E-mail: puzhen98@mail.ustc.edu.cn

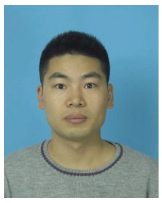

WANG Zhi-qiang (1990—), male, born in Bo-zhou, Anhui Province, PH.D, Associate Research Professor, he received his Ph.D from University of Science and Technology of China (USTC) in 2018, he mainly engaged in the field of laser beam propagation through random media and computational imaging. E-mail: zqwang@aiofm.ac.cn

FAN Cheng-yu (1965—), male, Ph.D., he is a researcher and doctoral supervisor at the Hefei Institutes of Physical Science, University of Science and Technology of China (USTC). His research primarily focuses on theoretical and experimental studies of atmospheric propagation of continuous and pulsed lasers, as well as investigations into the strong turbulence effects on laser propagation through the atmosphere. E-mail: cyfan@aiofm.ac.cn